

See discussions, stats, and author profiles for this publication at: <https://www.researchgate.net/publication/272126499>

Complex Structure of Ionic Liquids. Molecular Dynamics Studies with Different Cation–Anion Combinations

ARTICLE in JOURNAL OF CHEMICAL & ENGINEERING DATA · MAY 2014

Impact Factor: 2.04 · DOI: 10.1021/je500197x

CITATIONS

15

READS

23

3 AUTHORS, INCLUDING:



Jose Nuno A Canongia Lopes
Technical University of Lisbon

179 PUBLICATIONS 8,342 CITATIONS

[SEE PROFILE](#)

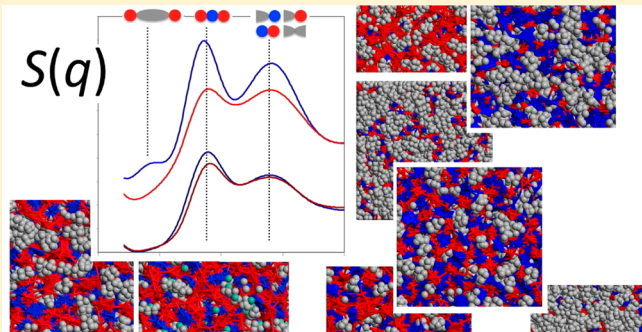
Complex Structure of Ionic Liquids. Molecular Dynamics Studies with Different Cation–Anion Combinations

Adilson A. Freitas,[†] Karina Shimizu,^{*,†} and José N. Canongia Lopes^{*,†,‡}

[†]Centro de Química Estrutural, Instituto Superior Técnico, Universidade de Lisboa, Avenida Rovisco Pais 1, 1049-001 Lisbon, Portugal

[‡]Instituto de Tecnologia Química e Biológica, Universidade Nova de Lisboa, Avenida da República, Estação Agronómica Nacional, 2780-157 Oeiras, Portugal

ABSTRACT: This article shows that the diverse structure and morphology of different ionic liquids can be interpreted using structure factor and radial distribution data. These two functions can be obtained using molecular dynamics (MD) simulation techniques. The lowest- q peaks of the structure factor spectra (prepeaks) can be assigned to characteristic separations between strands of the ionic liquid polar network that are mediated by nonpolar regions. On the other hand, the second lowest q -peaks reflect the medium-range ordering of the polar network itself. The systematic comparison between different groups of ionic liquids allows us to rationalize the relative amplitude and position of those peaks with the underlying structure of the ionic liquid and interpret such an outcome in terms of the relative size and nature of the corresponding ions.



one,^{7,8} or that there is no need to invoke micelle-like structures to account for the existence of a prepeak.⁹

The starting point for the present study will be a more detailed analysis of the structure and morphology of ILs where there are some sort of anomaly involving the existence or absence of the prepeak, namely, the study of the structural differences, first observed using X-ray diffraction, between 1-alkyl-3-methylimidazolium-based ILs, $[C_n\text{mim}][\text{Ntf}_2]$ ($n = 3, 6, 9$), and their counterparts with ether-substituted alkyl side chains, $[(C_1\text{OC}_1)_{(n/3)}\text{mim}][\text{Ntf}_2]$ ($n = 3, 6, 9$), cf. Scheme 1.

The focus of the study will then shift to the analysis of other features of the structure factor spectra, namely, the position and intensity of the peak appearing (or not) at q -values immediately above those of the prepeaks (cf. Figure 1a). This often overlooked “intermediate” peak has a close relation to the periodicity and nature of the polar network itself and will be used to check the relation between the ions that compose a given IL and the structure of its polar network. Again, the existence or absence of the intermediate peak will be used to infer the mesoscopic ordering of the IL and how different factors affect it. Since we will no longer need to deal directly with shorter or larger alkyl side chains (the focus will be on the charged parts of the ions that compose the polar network), the concept of homologous series (like those introduced in the previous paragraph) will be abandoned, and we will emphasize the differences between

Special Issue: Modeling and Simulation of Real Systems

Received: February 28, 2014

Accepted: April 30, 2014

Published: May 8, 2014

INTRODUCTION

Molecular dynamics (MD) simulations have been a privileged tool to probe the complex structure and properties of ionic liquids at an atomistic level. For instance, the first studies suggesting that ionic liquids are in fact nanosegregated fluids composed by a polar network permeated by nonpolar domains originated from MD studies.^{1–3} These were later corroborated by experimental X-ray diffraction studies⁴ that confirmed the possibility of extensive nonpolar domains formed by the alkyl side chains of some of the ions that constitute ionic liquids (ILs).

Most of those first studies were focused on the so-called prepeak of the corresponding structure factor spectra (Figure 1a), obtained either by experimental or simulation techniques. Such a prepeak has been associated with the characteristic length scales of the nonpolar regions that are able to effectively separate different “strands” of the polar network: when those nonpolar regions merge together and form a second continuous subphase able to percolate the entire fluid (together with the polar network they will define a bicontinuous morphology), a so-called prepeak appears at low q -values, which corresponds to the characteristic wavenumber of the two intermeshed regions.

Since the morphology of those nanosegregated regions is not directly accessible by experimental techniques some degree of controversy raged for sometime concerning the relation between the structure of the IL and the existence of prepeaks.^{5,6} The issue has been revisited many times, and it was found recently, for instance, that while the existence of long alkyl side chains is a necessary condition to produce prepeaks it is not a sufficient

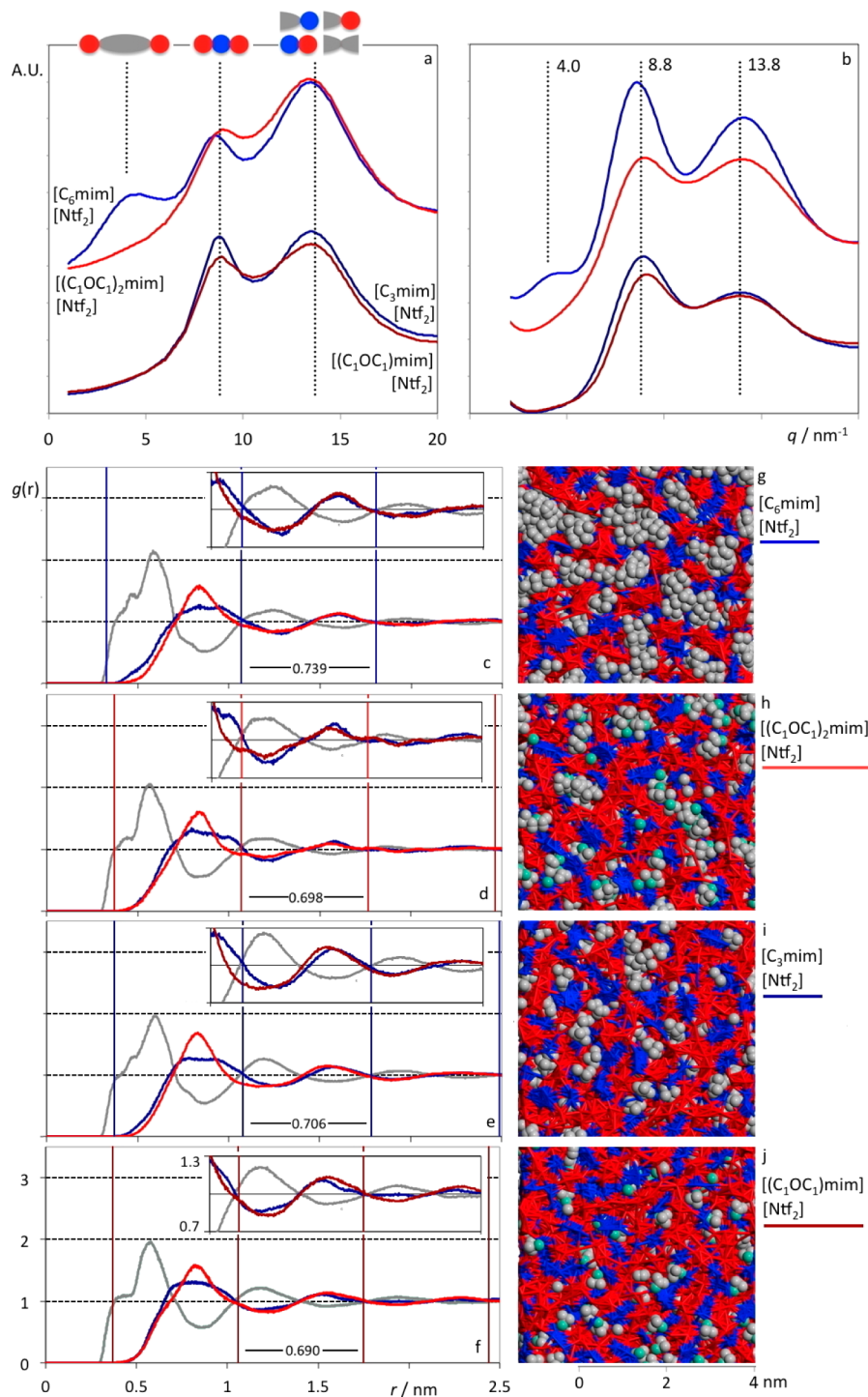


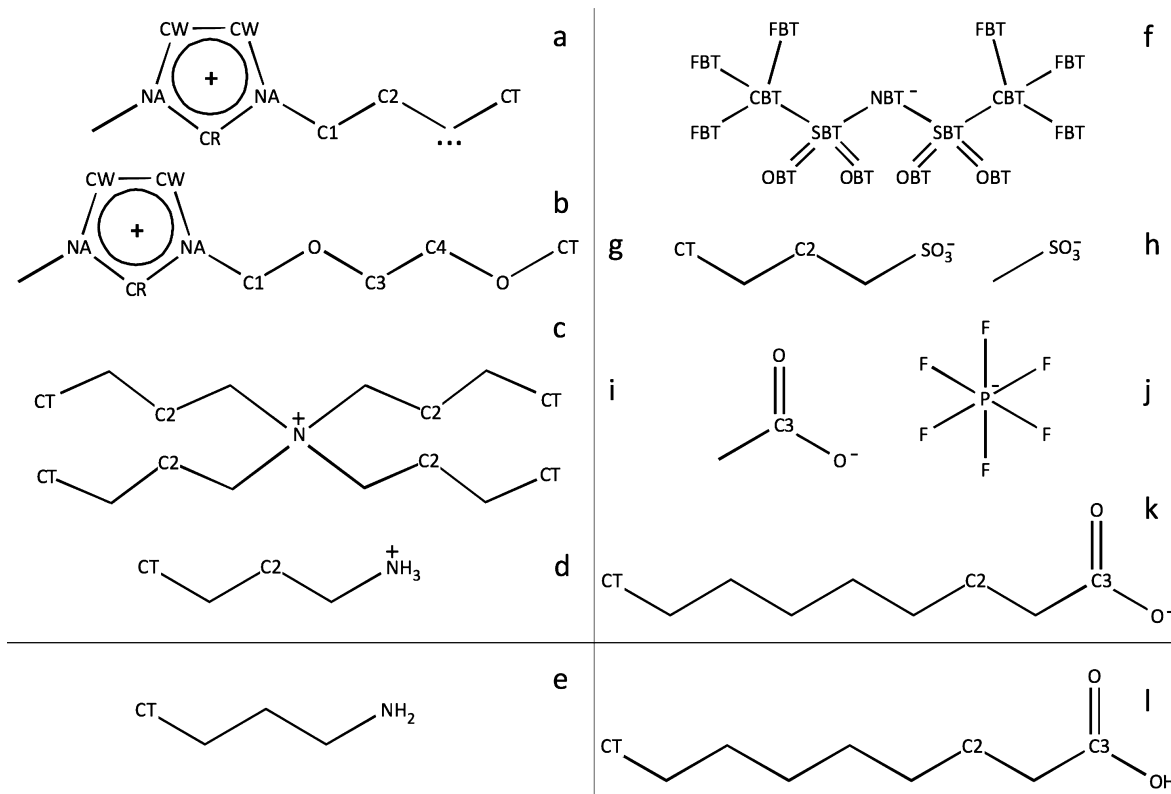
Figure 1. Structural data for imidazolium-based ionic liquids (ILs) with alkyl and glycol ether side chains. (a) Experimental (X-ray diffraction) structure factor spectra of $[C_6\text{mim}][\text{Ntf}_2]$, $[(C_1\text{OC}_1)\text{mim}][\text{Ntf}_2]$, $[C_3\text{mim}][\text{Ntf}_2]$, and $[(C_1\text{OC}_1)_2\text{mim}][\text{Ntf}_2]$. Figure adapted from ref 19. (b) MD simulation structure factor spectra. Systems as in previous panel. The vertical dotted lines marking the positions of the peaks are positioned at exactly the same values in both graphs; (c–f) radial distribution functions between the centroid of the imidazolium ring, CM, and the nitrogen atom, NBT, of the anion: CM–NBT in gray, NBT–NBT in red, CM–CM in blue. The colored vertical gridlines correspond to the characteristic d -spacing given by $2\pi/q$ of the structure factor intermediate q -peak; (g–j) simulation box: charged parts of the cation in blue, charged parts of the anion in red, alkyl side chains (C2 to CT) in gray, glycol ether side chains (C2 to CT) in gray/light green (ether oxygen atoms).

(i) ILs based on ions with a single long alkyl side chain (e.g., $C_n\text{mim}][\text{Ntf}_2]$ ($2 < n < 10$)) and those of a more symmetrical nature, like those based on the tetra-alkyl ammonium or tetra-alkyl phosphonium cations; (ii) protic versus aprotic ILs, (iii) ILs based on anions of different sizes, charge distribution, and flexibility. The discussion section will be subdivided accordingly.

EXPERIMENTAL SECTION

Molecular dynamics (MD) of condensed phases of different pure ILs and one molecular solvent were carried out using the DL-POLY package.¹⁰ All ions and molecules were modeled using a previously described all-atom nonpolarizable force field

Scheme 1. Structural Formulas and Atomic Nomenclature of the Cations (a–d) and Anions (f–k) of the Ionic Liquids Used in This Work, with Structural Formulas (e and l) Corresponding to the Two Neutral Species That Are the Conjugated Bases/Acids of the (d and k) Ions, Respectively



(CL&P),^{11–14} which is based on the OPLS-AA framework¹⁵ but was to a large extent developed specifically for ILs. The OPLS-AA parametrization was employed for the molecular solvent. When studying microstructured fluids, the size of the systems and the duration of the simulations are of particular importance since periodic boundary conditions can induce artificial finite-size effects on the length scales of the observed nanostructures. System sizes were chosen as to contain around 13,000 atoms, which correspond to cutoff distances above 1.6 nm and yielding cubic simulation boxes up to 125 nm³. The number of ion pairs and size of the box for all ILs and molecular solvents are presented in Table 1. Due to the slow dynamics of this type of system, special care was taken to ensure the attainment of equilibrium conditions: (i) equilibrations started from initial low-density configurations, with ions placed at random in periodic cubic boxes; (ii) typical equilibrations were implemented for more than 1 ns under *N*–*p*–*T* ensemble conditions (under the action of Nosé–Hoover barostats and thermostats); (iii) multiple re-equilibrations through the use of temperature annealing and switching off and on of the Coulomb interactions were performed; (iv) further simulation runs were used to produce equilibrated systems at the studied temperatures. The equilibrated systems were used in production runs of at least 4 ns. Electrostatic and repulsive-dispersive interactions were explicitly calculated for distances below the 1.6 nm cutoff. In the case of repulsive-dispersive interactions, long-range corrections were applied assuming the system had a uniform density beyond this cutoff radius. Long-range electrostatic interactions were treated using the Ewald summation method considering six reciprocal-space vectors.

The total static structure factors, $S(q)$, were computed according to a previously described methodology:⁷

Table 1. Studied Systems and Simulation Conditions (Size of the Equilibrated Boxes)^a

	N ion pairs	$V_{\text{box}}/\text{nm}^3$	l_{box}/nm	scheme
[C ₃ mim][Ntf ₂]	320	139.8	5.19	a, f
[C ₆ mim][Ntf ₂]	275	142.2	5.22	a, f
[(C ₁ OC ₁)mim][Ntf ₂]	350	147.2	5.28	b, f
[(C ₁ OC ₁) ₂ mim][Ntf ₂]	300	146.4	5.27	b, f
[C ₆ mim][C ₄ SO ₃]	280	136.5	5.15	a, g
[N ₄ 444][C ₄ SO ₃]	230	157.1	5.40	c, g
[C ₄ NH ₃][Ntf ₂]	1000	391.4	7.32	d, f
[C ₄ NH ₃][C ₁ COO]	1000	239.7	6.21	d, i
[C ₄ NH ₃][C ₈ COO]	1000	457.8	7.71	d, k
(C ₄ NH ₂ + C ₈ COOH)	1000 ^b	502.5	7.95	e, l
[C ₄ mim][Ntf ₂]	300	147.2	5.28	a, f
[C ₄ mim][C ₁ COO]	450	147.2	5.28	a, i
[C ₄ mim][C ₁ SO ₃]	410	146.4	5.27	a, h
[C ₄ mim][PF ₆]	410	153.1	5.35	a, j

^aThe last column refers to the corresponding structural formulas of the ions/molecules given in Scheme 1. ^bNumber of molecules of each type.

$$S(q) = \sum_i \sum_j S_{ij}(q) \quad (1)$$

$$S_{ij}(q) = \frac{\rho_o x_i x_j b_i(q) b_j(q) \int_0^R 4\pi r^2 [g_{ij}(r) - 1] \frac{\sin(qr)}{qr} \frac{\sin(\pi r)}{\pi r / R} dr}{(\sum_i x_i b_i(q))^2} \quad (2)$$

where $S_{ij}(q)$ is the partial static structure factor between atoms types *i* and *j* (e.g., between carbon, hydrogen, and/or nitrogen

atoms), calculated from the corresponding Fourier transforms of the partial radial distribution functions $g_{ij}(r)$; r is the distance; q is the scattering vector; ρ_0 is the average atom number density; R is the cutoff used in the calculation of the $g_{ij}(r)$ functions, set to half the size of the cubic simulation box; x_i and x_j are the atomic fraction of i and j ; and $b_i(q)$ and $b_j(q)$ are the coherent bound neutron scattering lengths of the corresponding atom type, interpolated from recommended values in the International Tables for Crystallography.¹⁶ The term $\sin(\pi R)/(\pi r/R)$ is a Lorch type window function¹⁷ that was added to eq 2 to reduce the effect of using a finite cutoff in the radial distribution function calculation.

■ RESULTS AND DISCUSSION

i. Vanishing Prepeaks Revisited: Alkyl versus Glycol-Ether Chains. Figure 1 shows the simulation results for the systems that include imidazolium-based cations with alkyl and glycol-ether chains. Since we wanted to compare any structural differences arising from the functionalization of the alkyl chain (substitution of one methylene ($-\text{CH}_2-$) group by a ether oxygen atom ($-\text{O}-$)), we decided to concentrate on data for $[\text{C}_3\text{mim}][\text{Ntf}_2]$ and $[\text{C}_6\text{mim}][\text{Ntf}_2]$ and their two functionalized counterparts with analogous side chain lengths $[(\text{C}_1\text{OC}_1)\text{mim}][\text{Ntf}_2]$ and $[(\text{C}_1\text{OC}_1)_2\text{mim}][\text{Ntf}_2]$, respectively. Unlike other members of the $[(\text{C}_1\text{OC}_1)\text{mim}][\text{Ntf}_2]$ homologous family, there is experimental structural data (X-ray diffraction results) for the two latter systems. The comparisons between such results and the structure factors obtained by simulation are depicted in Figures 1a (simulation) and 1b (experimental). Although the relative intensity of the peaks (the y-scale is in arbitrary units) differs between the experimental and simulated results the intensity trends among peaks is correctly conveyed, as well as (and most importantly) the corresponding q -values. In fact all structures in both graphs exhibit two peaks (the so-called intermediate peaks at q -values around 8.8 nm^{-1} and the so-called contact peaks at q -values around 13.8 nm^{-1}). As discussed in previous publications^{9,16} these reciprocal space peaks correspond in direct space to characteristic distances between atoms due to intramolecular and close contact intermolecular interactions (the contact peaks) and to the shortest separations between polar groups of the same charge (the intermediate peaks). These relations are depicted as the vignettes in Figure 1a.

Only the $[\text{C}_6\text{mim}][\text{Ntf}_2]$ system exhibits a small prepeak ($q = 4 \text{ nm}^{-1}$) that corresponds to the separation between polar groups separated by a nonpolar domain. The nonexistence of such prepeak for the other systems has been discussed^{7,17} in terms of the size and nature of the corresponding nonpolar domains. In $[\text{C}_3\text{mim}][\text{Ntf}_2]$ and $[(\text{C}_1\text{OC}_1)\text{mim}][\text{Ntf}_2]$ the side chains are too small to effectively separate different strands of the polar network and create characteristic separation lengths within the polar network of the IL. On the other hand, in $[(\text{C}_1\text{OC}_1)_2\text{mim}][\text{Ntf}_2]$ the side chain is as long as in $[\text{C}_6\text{mim}][\text{Ntf}_2]$ but, due to the presence of the oxygen atoms, it is able to interact more strongly with the polar network, and it can also adopt kinked conformations that allow the chain to fold back and explore with more freedom a much larger conformational phase space. These two characteristics of the glycol ether chains cause the sheathing of the polar network by the side chains, preclude their segregation into bulky nonpolar domains, and consequently suppress the existence of the so-called prepeak.

This was explored at length in a previous article⁷ so now we turn our attention to what is happening in terms of the intermediate peaks. Figure 1c–f represents the pair radial distribution

functions, $g(r)$, between selected atoms/positions in the charged parts of the cation and the anion of each system—the centroid of the imidazolium ring and the central nitrogen atom, NBT, of the $[\text{Ntf}_2]^-$ ion, respectively. The three lines in each graph represent cation–anion (gray), anion–anion (red), and cation–cation (blue) distribution functions. The opposition-of-phase behavior of the former lines is obvious relative to the two last ones. Moreover, if one takes the q -values from the intermediate peak of the corresponding structure-factor graphs (the corresponding q -values were obtained by peak deconvolution), converts them to direct-space characteristic lengths ($d = 2\pi/q$), builds grids with a characteristic spacing given by d , and superimposes the grids on the corresponding $g(r)$ graphs, one sees that the intermediate peak shows the periodicity of the polar network of each IL (alternation between ions of opposite and similar charge as one increases the distance from a given central ion). In all cases such periodic arrangement is still visible at distances above 2 nm, corresponding to correlations of atoms more than 6 ionic layers apart.

Figure 1c–f also shows that the spacing is not the same for the four ILs under discussion, albeit the fact that their polar moieties are all the same. The two alkylated ILs exhibit larger grid spacing relative to their glycol ether counterparts— d (Figure 1e) $>$ d (Figure 1f) and d (Figure 1c) $>$ d (Figure 1d); the ILs with longer side chains exhibit larger grid spacing relative to their shorter-chain counterparts— d (Figure 1c) $>$ d (Figure 1e) and d (Figure 1d) $>$ d (Figure 1f). This is in total agreement with the small deviations found in the corresponding q -value positions of the intermediate peaks (Figure 1a and b). This means that the so-called polar network of the ILs is perturbed (stretched) (i) as one increases the number of atoms in the (nonpolar) side chains of the cation or (ii) as one changes from the less segregated (sheathing) glycol ether chains to the alkyl ones. Such stretching-without-breaking is probably accomplished by the possibility of reorientation of the charged parts of the cations relative to each other (compare for instance the different morphologies of the first peaks in the $g(r)$ functions in Figure 1c–f). After all, the charged parts of both ions can establish contact via multiple competing points of interaction (e.g., any of the aromatic hydrogen atoms of the imidazolium ring of the cation; any of the oxygen atoms of the bis triflamide anion). In the case of the flexible bis triflamide anion the four oxygen atoms can also assume different relative orientations/distances toward each other,^{18–20} which will also add to the versatility/resilience of the corresponding polar network. In other words the polar networks of these particular ILs are able to adapt themselves to the presence of larger side chains and bulkier nonpolar domains without loosing their periodic character over relatively large distances (specially for a liquid). One final inference can be made at this point: the somewhat less intense intermediate peaks of the ILs with glycol ether chains relative to their alkyl analogues (and the less clear-cut opposition-of-phase character of the corresponding $g(r)$ functions in the $r > 2 \text{ nm}$ region, specially in Figure 1d) seem to indicate that the ordering of the polar network at longer distances is more affected by the more interactive glycol ether chains than by better segregated alkyl chains. These more “subdued” intermediate peaks will be analyzed in the next section, where a vanishing prepeak will be also be found.

ii. More Vanishing Prepeaks and Shifting Intermediate Peaks: Mono- versus Tetra-Alkyl Substituted Cations. In this section we will continue to use ILs based on a similar anion (butylsulfonate, $[\text{C}_4\text{SO}_3]^-$, instead of bis triflamide) combined with two different cations. In fact we will use again the $[\text{C}_6\text{mim}]^+$ cation used in the last section and confront it with a tetrabutyl

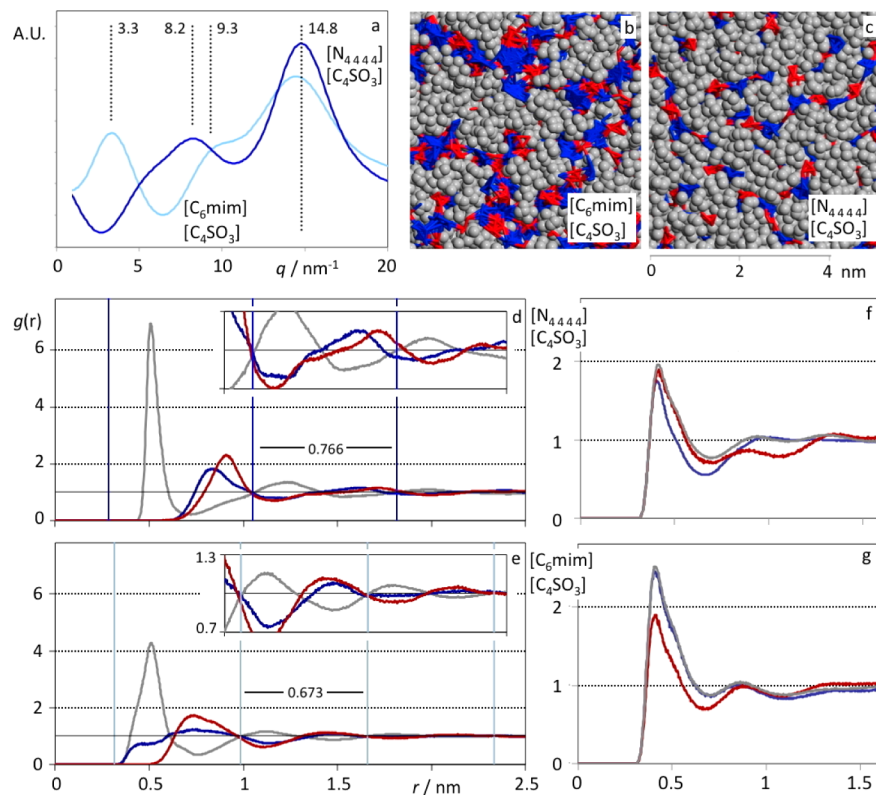


Figure 2. Structural data for imidazolium-based and tetra-alkyl ammonium-based ILs. (a) MD simulation structure factor spectra of $[\text{C}_6\text{mim}]^+[\text{C}_4\text{SO}_3]^-$ and $[\text{N}_{4444}]^+[\text{C}_4\text{SO}_3]^-$; (b,c) simulation box snapshots: charged parts of the cation in blue, charged parts of the anion in red, alkyl side chains (C2 to CT) in gray; (d,e) radial distribution functions, $g(r)$, between the centroid of the imidazolium ring, CM, or nitrogen atom of the tetra-alkyl ammonium cation, N, and the sulfur atom, S, of the anion: CM/N–S in gray, S–S in red, CM/N–CM/N in blue. The colored vertical gridlines correspond to the characteristic d -spacing given by $2\pi/q$ of the structure factor intermediate q -peak; (f,g) Radial distribution functions, $g(r)$, between the terminal carbon atoms of the alkyl chains, CT: CT(cation)–CT(anion) as gray lies, CT(anion)–CT(anion) as red lines, and CT(cation)–CT(cation) as blue lines.

ammonium cation, $[\text{N}_{4444}]^+$ (Clarification: 1-hexyl-3-methylimidazolium is obviously a cation substituted with two alkyl chains; the “mono-alkyl” in the title of this sub-section refers to its long alkyl chain (i.e., other than its methyl group)).

Before comparing the mono- versus tetra-alkyl effect, we will first discuss the structure factor of $[\text{C}_6\text{mim}]^+[\text{C}_4\text{SO}_3]^-$ (Figure 2a, light blue line) relative to that of $[\text{C}_6\text{mim}]^+[\text{Ntf}_2]^-$ (previous section, Figure 1a and b, blue lines). In both cases we have a prepeak that is more intense and shifted toward lower q -values (3.3 nm^{-1} instead of 4.0 nm^{-1}) than in the case of $[\text{C}_6\text{mim}]^+[\text{C}_4\text{SO}_3]^-$. This data is consistent with larger and bulkier nonpolar domains in $[\text{C}_6\text{mim}]^+[\text{C}_4\text{SO}_3]^-$ than in $[\text{C}_6\text{mim}]^+[\text{Ntf}_2]^-$ (compare the snapshots of Figures 2b and 1g). The difference between the two ILs lies of course in the anions: $[\text{C}_4\text{SO}_3]^-$ has an alkyl side chain that can be segregated together with those of the cation and participate in the formation of larger nonpolar domains. Such a fact can be confirmed by the inspection of the radial distribution functions of the CT–CT pair (the carbon atoms of the methyl groups at the end of hexyl and butyl alkyl chains in $[\text{C}_6\text{mim}]^+$ and $[\text{C}_4\text{SO}_3]^-$, respectively) depicted in Figure 2g. The blue line represents the pair correlations between CT atoms from the cation, the red line the pair correlation from CT atoms belonging to the anion, and the gray line correlation between pairs of CT atoms one belonging to the anion and the other to the cation. The graph shows that there is indeed a tendency for the C4 chains of the anion to be included in the domains formed by the C6 chains of the cation. The reverse, C6 chains in the smaller C4 domains, is not so probable—lower red line—probably due to size effects. The observed prepeak trend is also consistent with what happens in the $[\text{C}_n\text{mim}]^+[\text{Ntf}_2]^-$ homologous series.

homologous series: as the monoalkyl chains get longer, they form larger and bulkier nonpolar domains that produce more intense prepeaks that are shifted to lower q -values. The difference between the $[\text{C}_n\text{mim}]^+[\text{Ntf}_2]^-$ series and $[\text{C}_6\text{mim}]^+[\text{C}_4\text{SO}_3]^-$ case is that instead of having the chain exclusively in the cation, in the latter IL the alkyl moieties are part of both ions.

The intermediate peak also shifts when one compares $[\text{C}_6\text{mim}]^+[\text{C}_4\text{SO}_3]^-$ with $[\text{C}_6\text{mim}]^+[\text{Ntf}_2]^-$: the well-defined and intense intermediate peak around 8.8 nm^{-1} of the latter case (Figure 1a and b, blue lines) shifts to 9.3 nm^{-1} and becomes a shoulder in the former case (Figure 2a, light blue line). Such a shift means that the polar network is more compact (interionic distances between ions of the same sign are smaller, cf. grids in Figures 1c and 2e), and such a fact can be explained by the smaller dimensions of the polar head of the anion (the sulfonate group) when compared with the bis(trifluoromethyl) anion (at least the central part of it, composed by the amide nitrogen and its two sulphonyl groups). The lower intensity of the intermediate peak can be thought of as a consequence of the larger nonpolar domains, that perturbs more the periodicity of the polar network (a trend also observed for the $[\text{C}_n\text{mim}]^+[\text{Ntf}_2]^-$ homologous series.¹⁶ The combination of lower intensities with shifts to higher q -values (and the corresponding approach to the contact peak) justifies the transformation of the intermediate peak into a shoulder at 9.3 nm^{-1} .

Changes are more dramatic when the $[\text{C}_6\text{mim}]^+$ cation is replaced by the $[\text{N}_{4444}]^+$ cation.

In the latter case the prepeak vanishes, and the intermediate peak shifts to lower q -values (8.2 nm^{-1}). The snapshots depicted in Figure 2b and c confirm that the nonpolar domains in

$[N_{4\ 4\ 4\ 4}][C_4SO_3]$ are more extensive than in $[C_6mim][C_4SO_3]$, but as in the case of the vanishing prepeaks in the ether glycol chains, they are less bulky and more closely intermeshed with the polar network.

The prepeak vanishes (or almost vanishes since it can still be perceived as a very tenuous shoulder of the intermediate peak around 5 nm^{-1}) because the alkyl side chains (i) are not long enough (only C4 in both ions) and (ii) evenly distributed around the charged center of the cation (sheathing effect of the four side chains of the $[N_{4\ 4\ 4\ 4}]^+$ cation). It must be stressed that the contact interactions within the polar network of the $[N_{4\ 4\ 4\ 4}][C_4SO_3]$ are between the oxygen atoms of the anion and the hydrogen atoms connected to the C1 atoms of the cation (those atoms belong to the polar network; as in the $[C_6mim]^+$ case, the nonpolar part of the alkyl side chains only starts to be considered from C2 to CT).

The sheathing effect by the carbon atoms closest to the nitrogen atom of the cation (C1, C2) can be recognized taking into account the $g(r)$ functions given in Figure 2d: the “gap” between the gray and the blue and red lines at distances around 0.7 nm corresponds to distances occupied by the carbon atoms surrounding the nitrogen atom, that acts as a spacer and prevents an approximation from all sides of the charged center of the anion (the sulfur atom) to that of the cation and imposes larger first cation–cation and anion–anion distances. The consequence of this state of affairs is a string-like polar network (like alternating ionic beads in a necklace, Figure 2c). This “thin” polar network which is in fact quite twisted due to the possibility of several interacting sites in each cation and anion head (the eight hydrogen atoms attached to the four C1 atoms of the cation; the three oxygen atoms in the cation) has a limited periodic spatial ordering relative to the $[C_6mim][C_4SO_3]$ case (compare Figure 2d and e in the 1.5–2.2 nm range). The intermediate peak is still there, but its intensity is more subdued relative to the other ILs discussed so far.

iii. Vanishing Intermediate Peaks: Protic versus Aprotic

ILs. The following stage is to consider ILs based on ammonium cations with a single long alkyl side chain, $[C_4NH_3]^+$. These are protic ILs that in some cases, depending on the nature of the anion, can participate in an acid–base reaction and be at equilibrium with the corresponding neutral species (the conjugate base and acid of the cation and anion, respectively). Figure 3 shows the structure factors, $g(r)$ s, and simulation snapshots for butylammonium combined with the bis triflameide, acetate, and nonanoate anions ($[C_4NH_3][Ntf_2]$, $[C_4NH_3][C_1COO]$, and $[C_4NH_3][C_8COO]$, respectively) as well as an equimolar mixture of butylamine, C_4NH_2 , and nonanoic acid, C_8COOH , the neutral conjugated system of $[C_4NH_3][C_8COO]$.

The $[C_4NH_3][Ntf_2]$ system exhibits structure factor peaks at 5.4, 9.1, and 14.0 nm^{-1} (Figure 3a) that correspond to the pre-, intermediate, and contact peaks already found and discussed for the previous systems. The existence of a (albeit small) prepeak for a system with only a C4 side chain can be justified by the small size of the cation polar head (the smallest so far). The small size of the tails also implies relatively thin nonpolar networks separating different strands of the polar network and a prepeak shifted to relatively large q -values (5.4 nm^{-1}). Direct observation of the simulation snapshot of Figure 3g shows that the polar network of this IL is composed by relatively small cationic polar heads “appended” to larger anionic counterparts. This apparently unstable configuration (the anions seem to be touching each other) can be easily explained taking into account the fact that the $[Ntf_2]^-$ anions possess two $-CF_3$ groups at their extremities

(which are generally not counted as nonpolar moieties) that can interact with each other (segregation of fluorinated groups is common in many crystalline and liquid phases). This does not mean that the charged center of the anions will lie together (the NBT–NBT correlation depicted in the $g(r)$ function depicted in Figure 3c (red line) shows distances (0.7 nm) larger than the anion–cation contacts (around and below 0.5 nm). These latter contacts exhibit a rather complex correlation curve (gray line of Figure 3c, compared with those of Figure 3c–f) caused by the disparity in size of the polar network components (the “appendage” of the small cationic heads).

Things get really interesting when the $[Ntf_2]^-$ anion is replaced by anions (carboxylates, $[C_nCOO]^-$ with a much smaller polar head. Figure 3a and b shows that in those cases the intermediate peak vanishes, and the corresponding correlation functions in Figure 3d and e show that, apart from the first two ionic shells, the periodicity of the polar network is absent (no opposition-of-phase behavior for distances larger than 0.7 nm, large difference in the cation–cation and anion–anion first peaks). This confirms the strong correlation between the existence/absence of an intermediate peak and the existence/absence of medium-range periodicity in the polar network of an IL.

The issue to be discussed at this point is of course the absence of such periodicity of the polar network. Figure 3h and i shows in fact that there is a polar network (each cation head is attached to an anion head and vice versa), and this is confirmed by the first peaks in the $g(r)$ functions of Figure 3d and e. The point now is to notice that the polar network is composed by small ionic heads (the $-NH_3$ and $-COO$ groups) interacting in a quite versatile fashion via electrostatics and hydrogen-bonding with very little hindrance from surrounding nonpolar groups. This means that we have a necklace-like polar network that is extremely thin and flexible in the midst of nonpolar regions that even with only C4 chains occupy a relatively large proportion of the available volume. Such a fact will hinder the emergence of any intermediate-range ordering/periodicity.

The absence of the intermediate peaks for the $[C_4NH_3][C_1COO]$ and $[C_4NH_3][C_8COO]$ also has the added bonus of showing quite accurately the position of the prepeak. Obviously the q -value of the former system is larger (5.4 nm^{-1}) than that of the latter (3.8 nm^{-1}) due to the simple fact that the nonpolar domains are bulkier in $[C_4NH_3][C_8COO]$ (C8 plus C4 chains) than in $[C_4NH_3][C_4COO]$ (C4 plus C4 chains). The “clean” prepeak of $[C_4NH_3][C_4COO]$ also helps to corroborate the possible existence of a weak shoulder in $[N_{4\ 4\ 4\ 4}][C_4SO_3]$: as inferred in the previous section, that shoulder is assumed to exist around 5 nm^{-1} , not so far from the characteristic distances of C4 nonpolar domains.

The final issue to be discussed in this section is the possibility of any protic liquid to exist as a mixture of ions and neutral molecules due to the possibility of an acid–base equilibrium between species. In order to explore such situation we have decided to model a system representing the other extreme of the protic $[C_4NH_3][C_8COO]$ equilibrium: $C_4H_9NH_3^+ + C_8COO^- \rightleftharpoons C_4H_9NH_2 + C_8COOH$. The structure factor and $g(r)$ functions of an equimolar mixture of butyl-amine ($N_{4\ 0\ 0}$) and nonanoic acid (C_8COOH) is represented in Figure 3b and f. The corresponding simulation snapshot is given in Figure 3j. Figure 3f shows that there is even a loss of correlation even at shorter distances (earlier flatout) and that the first peak does not represent a cross-interaction between the two types of molecule but rather amine–amine interactions. In other words instead of the spatially unorganized polar network of $[C_4NH_3][C_8COO]$ we have no

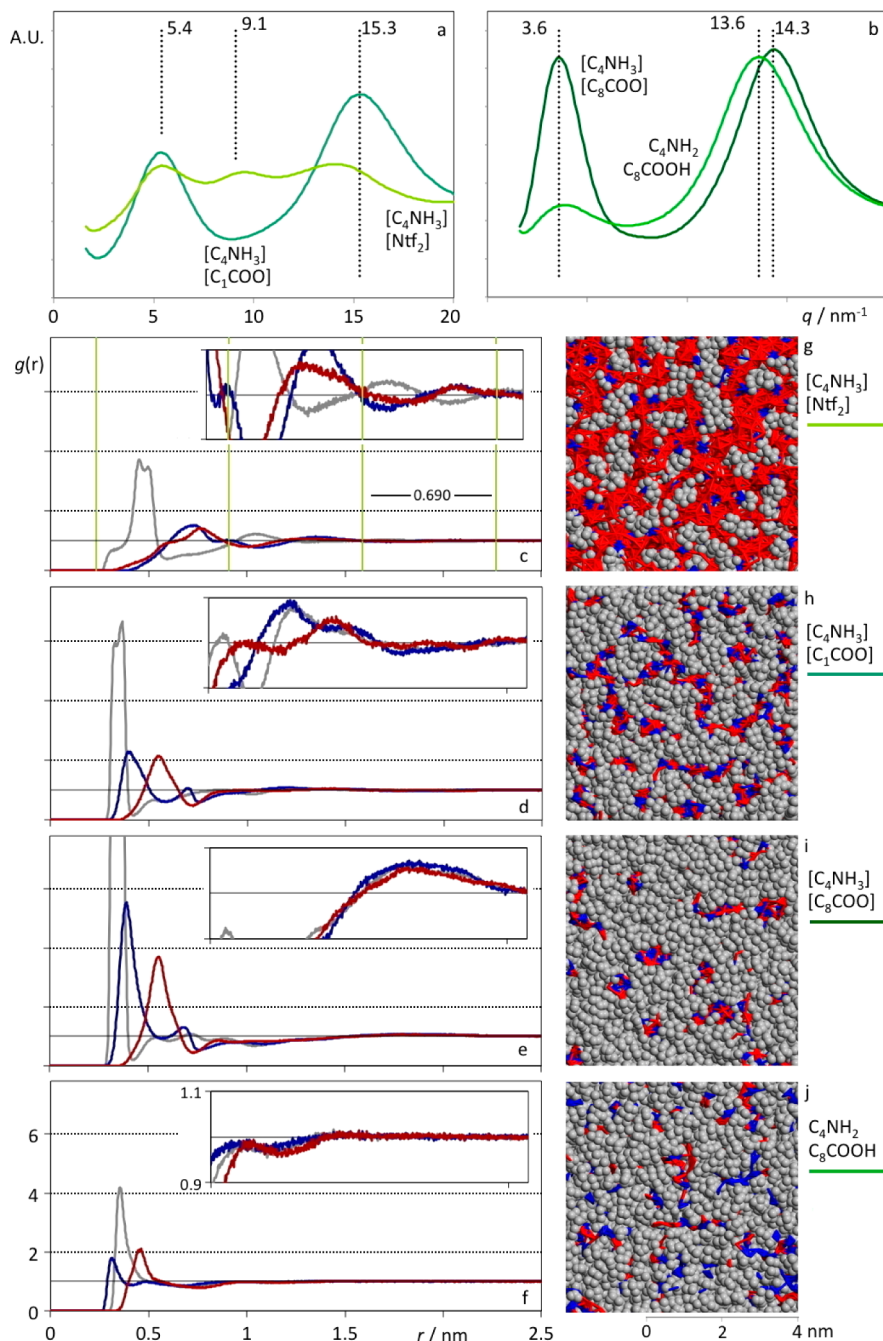


Figure 3. Structural data for butyl-ammonium-based ILs with different counterions and for the equimolar mixture of butylamine and nonanoic acid. (a,b) MD simulation structure factor spectra of $[C_4NH_3][Ntf_2]$, $[C_4NH_3][C_1COO]$, $[C_4NH_3][C_8COO]$, $(C_4NH_2 + C_1COOH)$; (c–f) radial distribution functions between the nitrogen atom, N, of ammonium/amine and the carbonyl carbon atom, C3, of carboxylate/carboxylic acid: N–C3 in gray, C3–C3 in red, N–N in blue. The colored vertical gridlines correspond in c to the characteristic d -spacing given by $2\pi/q$ of the structure factor intermediate q -peak; (g–i) simulation box snapshots: charged parts of the cation in blue, charged parts of the anion in red, alkyl side chains (C2 to CT) in gray; (j) simulation box snapshot: $-\text{CH}_2\text{NH}_2$ in blue, $-\text{CH}_2\text{COOH}$ in red, and alkyl chains (C2 to CT) in gray.

polar network, just specific interactions between the functional groups of the molecules. Interestingly, since the functionalized heads of the molecules perform specific interactions and the tails will be somewhat segregated, there is still a subdued prepeak relative to that of $[C_4NH_3][C_8COO]$, cf. Figure 3j with Figure 3i and also the structure factors in Figure 3b.

The snapshots in Figure 3i and j also show that the overall morphology of the two systems (nonpolar versus polar/functional) is not so distant. The structure of the real protic liquid (in equilibrium with a fraction of its conjugated neutral

species) will probably exhibit a morphology between the two extreme cases just presented.

iv. A Plethora of Peaks: An Anionic Menagerie. This last section focuses on the substitution of the anion of a given IL rather than the effects associated with the nature of the cation (including the length, functionalization, number, or inexistence of its alkyl side chains). In order to do that we have selected the $[C_4\text{mim}]^+$ cation and combined it with four different anions. It is important to stress that ILs exhibit a much larger variety in terms of their possible anions than the corresponding cations. We

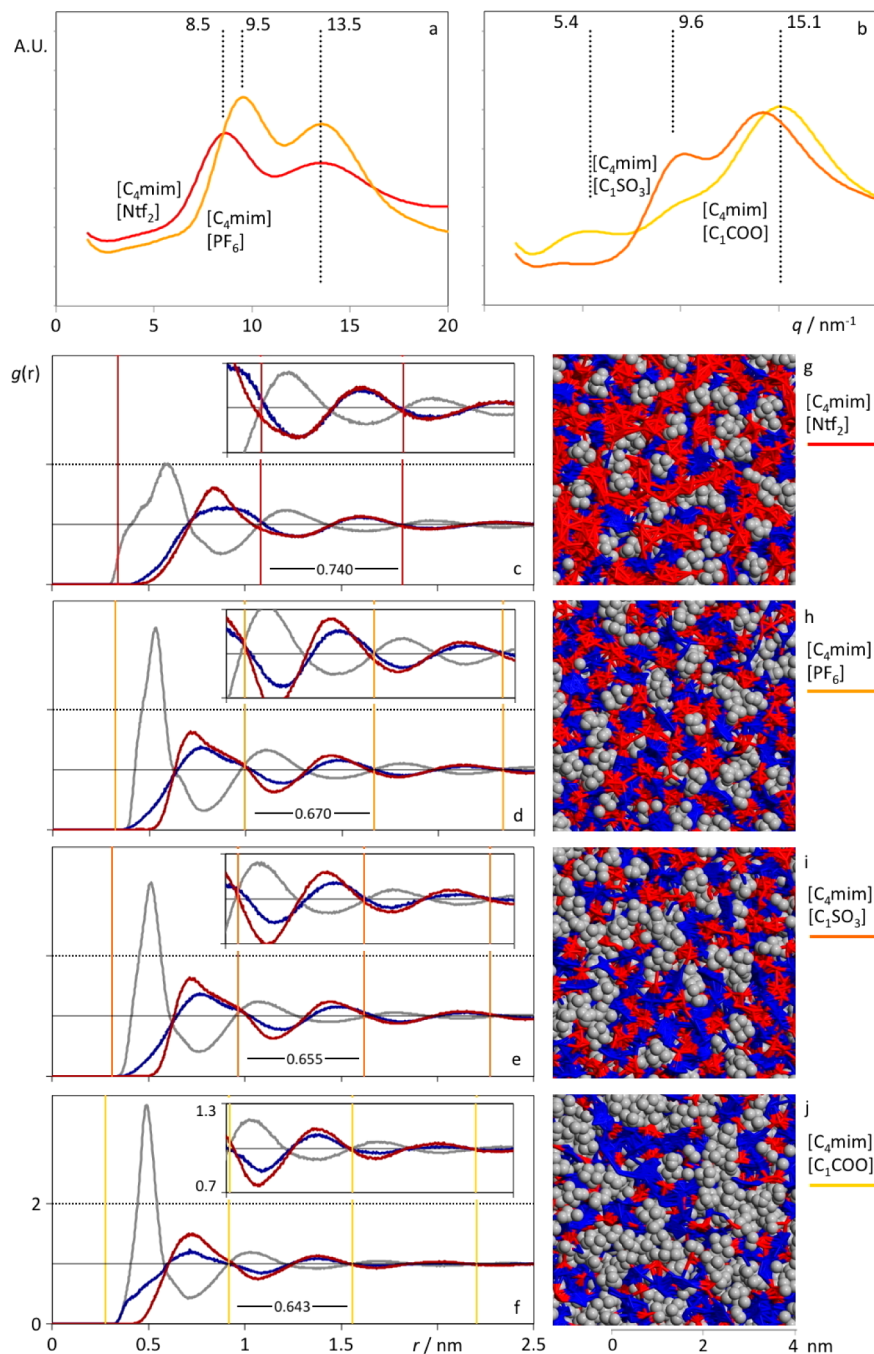


Figure 4. Structural data for 1-butyl-3-methylimidazolium-based ILs with different anions. (a,b) MD structure factor spectra of $[C_4\text{mim}]^+ [N\text{tf}_2]^-$, $[C_4\text{mim}]^+ [P\text{F}_6]^-$, $[C_4\text{mim}]^+ [C_1\text{SO}_3]^-$, and $[C_4\text{mim}]^+ [C_1\text{COO}]^-$; (c–f) radial distribution functions between the centroid of the imidazolium ring, CM, and the NBT/P/S/C3 atoms of the anions (cf. Scheme 1): CM–NBT/P/S/C3 in gray, NBT/P/S/C3–NBT/P/S/C3 in red, CM–CM in blue. The colored vertical gridlines correspond to the characteristic d -spacing given by $2\pi/q$ of the structure factor intermediate q -peak; (g–j) simulation box snapshots: charged parts of the cation in blue, anions in red, cation alkyl side chains (C2 to CT) in gray.

chose the $[C_4\text{mim}]^+$ cation as an ion whose alkyl side chains will form nonpolar domains with sizes that will not produce large prepeaks. The selected anions do not exhibit large alkyl chains for the same reason. It is important to stress that the selected anions do not form any particular homologous series. This means that it will not be possible to discuss the $S(q)$ peaks in terms of systematic trends. However, we will attempt to find relationships between the different peaks and the diverse nature of the anions.

Figure 4a and b shows the structure factors for the four selected ILs. As expected the prepeaks are almost absent in all

situations—larger anions such as $[N\text{tf}_2]^-$ or $[P\text{F}_6]^-$ show flattened regions around 5 nm^{-1} (typical of C4 domains); smaller anions such as $[C_1\text{SO}_3]^-$ or $[C_1\text{COO}]^-$ show very small peaks in the same region.

On the other hand, the intermediate peaks vary considerably, from strong peaks in $[C_4\text{mim}]^+ [N\text{tf}_2]^-$ centered around 8.5 nm^{-1} to increasingly more subdued peaks centered around 9.5 nm^{-1} for $[C_4\text{mim}]^+ [P\text{F}_6]^-$, $[C_4\text{mim}]^+ [C_1\text{SO}_3]^-$, and $[C_4\text{mim}]^+ [C_1\text{COO}]^-$. These are consistent with the corresponding $g(r)$ functions depicted in Figure 4c to f that show a larger grid spacing for the

larger polar moieties of the $[\text{Ntf}_2]^-$ anion. Otherwise the $g(r)$ functions also show that more subdued intermediate peaks correspond to less intense correlations of the polar network in ionic shells further away from the central ion (compare for instance the height of the peaks and troughs in the insets of Figure 4c–f, all up to the fifth and sixth ionic shells of a given ion). The smallest ion (acetate) is the one exhibiting the more subdued intermediate peak, a situation that is coherent with its vanishing if the $[\text{C}_4\text{mim}]^+$ cation is also replaced by a smaller cation like $[\text{C}_4\text{NH}_3]^+$ (cf. previous section). Ionic liquids based on dicyanamide, $[\text{N}(\text{CN})_2]^-$ (also a small anion), also exhibit structure factors with very small intermediate peaks (not shown in this paper).

Several factors can influence the degree of structuration of the polar network, namely, the size of the anions (and concomitantly the ratio between nonpolar and polar regions), the number and distribution of the centers of negative charge around the anion (e.g., four conformationally flexible oxygen atoms, OBT, in $[\text{Ntf}_2]^-$ versus six evenly distributed and fixed F atoms in $[\text{PF}_6]^-$), the overall symmetry of the anion (e.g., central or semicentral in $[\text{PF}_6]^-$ and $[\text{Ntf}_2]^-$, head–tail in $[\text{C}_1\text{SO}_3]^-$ or $[\text{C}_1\text{COO}]^-$, and the possibility of simultaneous attachment to different cations (e.g., it will be harder for $[\text{C}_1\text{COO}]^-$ to bridge several cations than for $[\text{Ntf}_2]^-$).

CONCLUSIONS

The unique properties of ILs must reflect in some way their complex nanosegregated structures. Such structures can be modeled and studied using MD simulation techniques.

The present contribution showed that there is an enormous variety of types of structure/morphology among common ILs and that such a variety can be interpreted in terms of the main features of the corresponding structure factor spectra and selected $g(r)$ correlation functions.

The so-called prepeaks of the structure factor spectra of most ILs can be assigned to characteristic separations between strands of their polar network that are mediated by nonpolar regions. On the other hand the so-called intermediate peaks reflect the medium-range ordering of the polar network of the ILs.

By comparing in a systematic way different groups of ILs, we were able to rationalize the relative amplitude and position of those peaks with the corresponding underlying structure and interpret such an outcome in terms of the relative size and nature of the ions that compose a given IL. Important issues unveiled in this way include: (i) the suppression of the prepeaks when the alkyl side chains of ILs are either too small (below C5–C6), too interactive (glycol-like chains), or wrap around the ionic centers (tetra-alkyl ammonium cations); (ii) the slight expansion of the alternating layers of the polar network (accompanied by shifts of the intermediate peaks to lower q -values) caused by the growth of the nonpolar regions. This “stretch” of the polar network can be accompanied by rearrangements of the charged parts of the ions within it; (iii) the suppression of the spatial ordering of the polar network for ions that are small and can have multiple interaction centers (alkylammonium in protic ILs). This can culminate in the (partial) destruction of the polar network itself when the protic ILs revert to the corresponding neutral species; (iv) the main features of the $S(q)$ spectra can be masked by the superimposition of peaks (shifts due to the absolute or relative size of the charged parts of the ions and their relation to the size of the nonpolar moieties): a small alkyl side chain that does not produce a prepeak in the presence of bulky ionic moieties can do so in the presence of smaller ions; the pre and intermediate peaks

can partially merge when small tails are combined with bulky ion heads.

AUTHOR INFORMATION

Corresponding Authors

*K.S.: E-mail: karina.shimizu@ist.utl.pt.

*J.N.C.L.: E-mail: jnlopes@ist.utl.pt.

Funding

Financial support provided by Fundação para a Ciência e Tecnologia (FCT) through projects FCT-ANR/CTM-NAN/0135/2012 (including a postdoctoral grant of KS), PTDC/QUI-QUI/117340/2010, and PEst-OE/QUI/UI0100/2013.

Notes

The authors declare no competing financial interest.

REFERENCES

- (1) Urahata, S. M.; Ribeiro, M. C. C. Structure of ionic liquids of 1-alkyl-3-methylimidazolium cations: A systematic computer simulation study. *J. Chem. Phys.* **2004**, *120*, 1855–1863.
- (2) Wang, Y.; Voth, G. A. Unique Spatial Heterogeneity in Ionic Liquids. *J. Am. Chem. Soc.* **2005**, *127*, 12192–12193.
- (3) Pádua, A. A. H.; Canongia Lopes, J. N. Nanostructural Organization in Ionic Liquids. *J. Phys. Chem. B* **2006**, *110*, 3330–3335.
- (4) Triolo, A.; Russina, O.; Bleif, H.; Di Cola, E. Nanoscale Segregation in Room Temperature Ionic Liquids. *J. Phys. Chem. B* **2007**, *111*, 4641–4644.
- (5) Hardacre, C.; Holbrey, J. D.; Mullan, C. L.; Youngs, T. G. A.; Bowron, D. T. Small angle neutron scattering from 1-alkyl-3-methylimidazolium hexafluorophosphate ionic liquids ($[\text{C}_n\text{mim}][\text{PF}_6]$, $n = 4, 6$, and 8). *J. Chem. Phys.* **2010**, *133*, 74510–74517.
- (6) Triolo, A.; Russina, O.; Fazio, B.; Triolo, R.; Di Cola, E. Morphology of 1-alkyl-3-methylimidazolium hexafluorophosphate room temperature ionic liquids. *Chem. Phys. Lett.* **2008**, *457*, 362–365.
- (7) Shimizu, K.; Bernardes, C. E. S.; Triolo, A.; Canongia Lopes, J. N. Nano-segregation in ionic liquids: scorpions and vanishing chains. *Phys. Chem. Chem. Phys.* **2013**, *15*, 16256–16262.
- (8) Pereiro, A. B.; Gallego, M. J. P.; Shimizu, K.; Marrucho, I. M.; Canongia Lopes, J. N.; Piñeiro, M. M.; Rebelo, L. P. N. On the Formation of a Third, Nanostructured Domain in Ionic Liquids. *J. Phys. Chem. B* **2013**, *117*, 10826–10833.
- (9) Annapureddy, H. V. R.; Kashyap, H. K.; De Biase, P. M.; Margulis, C. J. What is the Origin of the Prepeak in the X-ray Scattering of Imidazolium-Based Room-Temperature Ionic Liquids? *J. Phys. Chem. B* **2010**, *114*, 16838–16846.
- (10) Smith, W.; Forester, T. R. *The DL_POLY Package of Molecular Simulation Routines (v.2.2)*; The Council for The Central Laboratory of Research Councils; Daresbury Laboratory: Warrington, U.K., 2006.
- (11) Canongia Lopes, J. N.; Deschamps, J.; Pádua, A. A. H. Modeling ionic liquids using a systematic all-atom force field. *J. Phys. Chem. B* **2004**, *108*, 2038–2047.
- (12) Canongia Lopes, J. N.; Pádua, A. A. H. Molecular Force Field for Ionic Liquids Composed of Triflate or Bistriflylimide Anions. *J. Phys. Chem. B* **2004**, *108*, 16893–16898.
- (13) Canongia Lopes, J. N.; Pádua, A. A. H. Molecular force field for ionic liquids. III: Imidazolium, pyridinium and phosphonium cations; bromide and dicyanamide anions. *J. Phys. Chem. B* **2006**, *110*, 19586–19592.
- (14) Canongia Lopes, J. N.; Pádua, A. A. H.; Shimizu, K. Molecular Force Field for Ionic Liquids IV: Trialkylimidazolium and Alkoxycarbonyl-Imidazolium Cations; Alkylsulfonate and Alkylsulfate Anions. *J. Phys. Chem. B* **2008**, *112*, 5039–5046.
- (15) Jorgensen, W. L.; Maxwell, D. S.; Tirado-Rives, J. Development and Testing of the OPLS All-Atom Force Field on Conformational Energetics and Properties of Organic Liquids. *J. Am. Chem. Soc.* **1996**, *118*, 11225–11236.
- (16) Brown, P. J.; Fox, A. G.; Maslen, E. N.; O’Keefe, M. A.; Willis, T. M. In *International Tables for Crystallography*; Prince, E., Ed.;

International Union of Crystallography: Chester, England, 2006; Vol. C, ch 6.1, pp 554–595.

(17) Lorch, E. A. Neutron diffraction by germania, silica and radiation-damaged silica glasses. *J. Phys. C: Solid State Phys.* **1969**, *2*, 229–237.

(18) Shimizu, K.; Bernardes, C. E. S.; Canongia Lopes, J. N. Structure and Aggregation in the 1-Alkyl-3-Methylimidazolium Bis-(trifluoromethylsulfonyl)imide Ionic Liquid Homologous Series. *J. Phys. Chem. B* **2014**, *118*, 567–576.

(19) Triolo, A.; Russina, O.; Caminiti, R.; Shirota, H.; Lee, H. Y.; Santos, C. S.; Murthy, N. S.; Castner, E. W. Comparing intermediate range order for alkyl- vs. ether-substituted cations in ionic liquids. *Chem. Commun.* **2012**, *48*, 4959–4961.

(20) Canongia Lopes, J. N.; Shimizu, K.; Pádua, A. A. H.; Umebayashi, Y.; Fukuda, S.; Fujii, K.; Ishiguro, S. A Tale of Two Ions: The Conformational Landscapes of Bis(trifluoromethanesulfonyl)amide and N,N-Dialkylpyrrolidinium. *J. Phys. Chem. B* **2008**, *112*, 1465–1472.

(21) Fujii, K.; Fujimori, T.; Takamuku, T.; Kanzaki, R.; Umebayashi, Y.; Ishiguro, S. I. Conformational Equilibrium of Bis(trifluoromethanesulfonyl) Imide Anion of a Room-Temperature Ionic Liquid: Raman Spectroscopic Study and DFT Calculations. *J. Phys. Chem. B* **2006**, *110*, 8179–8183.

(22) Johansson, P.; Gejii, S. P.; Tegenfeldt, J.; Lindgren, J. The imide ion: potential energy surface and geometries. *Electrochim. Acta* **1998**, *43*, 1375–1379.